

Olfactory Mucosa of the South American Armadillo *Chaetophractus villosus*: An Ultrastructural Study

CARINA C. FERRARI, HERNÁN J. ALDANA MARCOS,
PABLO D. CARMANCAHI, AND JORGE M. AFFANNI*

Instituto de Neurociencia (INEUCI-CONICET-UBA), Facultad de Ciencias Exactas y Naturales, Ciudad Universitaria, Pab. II, 4 piso, LAB. 53, (1428), Buenos Aires, Argentina

ABSTRACT

The sense of olfaction in armadillos plays an important role, suggested by the great development of the nasal structures, olfactory bulbs, and related brain regions. The mammalian olfactory mucosa is a privileged site of neuronal death and regeneration during the whole life span. A detailed knowledge of its ultrastructure is convenient for gaining insight into the factors controlling those phenomena. We performed this work in species not previously studied in order to provide a firm basis for further research on those factors. No information is available on the histology and ultrastructure of the olfactory mucosa in the order Xenarthra to which armadillos belong.

Samples from the endoturbinals of the armadillo *Chaetophractus villosus* were prepared for light and electron microscopic examination by the usual conventional means. The olfactory epithelium of *Chaetophractus villosus* shows the classical three types of cells: supporting cells, olfactory receptor neurons, and basal cells. The olfactory neurons and the basal cells were similar to that described in other species. Two different types of supporting cells are described. An outstanding characteristic of the supporting cells is the normal presence of abundant phagosomes, apical secretory granules, apocrine-like protrusions, and highly developed smooth endoplasmic reticulum. Apoptotic bodies are frequently found in the infranuclear cytoplasm of supporting cells. The ductular epithelium of Bowman's glands reveals secretory activity. The lamina propria shows mixed Bowman's glands. Great development of smooth endoplasmic reticulum is observed in the mucous acinar cells. Evidence for merocrine and apocrine mechanisms in the Bowman's glands is presented.

The presence of apoptotic bodies and phagosomes in supporting cells suggests a participation in the cellular events induced by cell death and proliferation of the olfactory epithelium. The variety of characteristics exhibited by the supporting cells of the olfactory mucosa may contribute to a deeper understanding of their scarcely known functions. *Anat. Rec.* 252: 325–339, 1998. © 1998 Wiley-Liss, Inc.

Key words: olfactory mucosa; armadillo; Xenarthra; electron microscopy; apocrine secretion; apoptosis; supporting cells

The olfactory mucosa (OM) of vertebrates consists of two layers: a sensory olfactory epithelium (OE) and a deeper lamina propria with Bowman's glands (BG) and bundles of unmyelinated olfactory nerves immersed into a scanty connective tissue. The OM of mammals lines the dorsal and posterior surfaces of the nasal cavity (Allison, 1953). The OE consists of three basic cell types: olfactory receptor neurons (ORN), supporting cells (SC), and basal cells (BC; Allison, 1953; Graziadei, 1973). There are detailed electron microscopy studies of the OE in several species. The

pattern of histological organization is similar throughout most mammals (Graziadei, 1973; Graziadei and Monti-

Grant sponsor: National Research Council (CONICET-ARGENTINA).

*Correspondence to: Jorge M. Affanni, INEUCI-CONICET, Ciudad Universitaria Pab. II, 4 piso, Lab. 102 (1428), Buenos Aires, Argentina. E-mail: carina@bg.fcen.uba.ar

Received 7 January 1998; Accepted 29 April 1998

Graziadei, 1979; Farbman, 1992; Morrison and Costanzo, 1992; Morrison and Moran, 1995). In spite of the common pattern, the OM of different vertebrate species shows many morphological variations.

Special attention is being increasingly focused on the OM on account of several peculiar characteristics of biological relevance. The ORN are the only neurons in direct physical contact with the environment (Lewis and Dahl, 1995). In mammals, those neurons are continuously regenerated during adult life (Graziadei and Monti Graziadei, 1979). Several materials are transported from the OM to the olfactory bulb (Baker, 1995). The materials can subsequently be transported in both anterograde and retrograde directions within the central nervous system (Dahl and Hadley, 1991; Baker, 1995). Additionally, the OM shows high levels of xenobiotic metabolizing enzyme activity (Lewis and Dahl, 1995). On the other hand, cells of the immune system were found in the OM and immunoglobulins and cytoquines have been detected in nasal secretions (Mellert et al., 1992).

The BG deserve special attention because they produce the mucus layer, associated with olfactory transduction (Farbman, 1992; Getchell and Getchell, 1992), xenobiotic enzymes (Lewis and Dahl, 1995), and several olfactory binding proteins that facilitate transport of odorants to the ORN (Dear et al., 1991). Additionally, their cells express the mRNA for transforming growth factor α , which can stimulate division in the OE and production of at least some new ORN (Farbman and Buchholz, 1996).

The above-mentioned properties show that the OM is an active site of important phenomena. This points out the need of renewed research dedicated to this structure. Consequently, studies on animals not yet studied may be rewarding. Regarding this point, no representatives of the order Xenarthra were studied. The mammalian order Xenarthra (Edentata) include tree sloth, anteaters, and armadillos. The Xenarthra are eutherians, but they exhibit rather peculiar morphological and physiological characters, some of which are conservative (Eisenberg, 1981; Wetzel, 1985). Molecular studies indicate that the Xenarthra diverged from other eutherians nearly at the same time as the marsupial-eutherians split occurred (Engelmann, 1985; Novacek, 1994). This is why some authors (Mc Kenna, 1975; Novacek, 1994) suggested that xenarthrans represent the sister group to all other placental mammals.

Armadillos are valuable models for studies on the olfactory system (Affanni and Garcia Samartino, 1984; Ferreira-Moyano and Cinelli, 1986; Affanni et al., 1987). They are macrosmatic animals (Grassé, 1955). The sense of olfaction plays an important role suggested by the great development of the nasal structures (Ferrari, 1997), olfactory bulbs, olfactory tubercles, and large pyriform cortex (Benítez et al., 1994).

The aim of this paper is to describe the histological and ultrastructural composition of the OM in the South American armadillo *Chaetophractus villosus*.

MATERIALS AND METHODS

Eighteen Armadillos *Chaetophractus villosus* (10 females and 8 males) were used. The animals were maintained under standard laboratory conditions (light/dark cycle of 12 hours; 21°C of temperature; pellet food and water ad libitum). They were anesthetized with ketamine

hydrochloride (40 mg/Kg, i.m.) and sodium thiopental (60 mg/Kg, i.p.) and sacrificed during spring, summer, autumn, and winter. The OM of some animals was fixed by perfusion, whereas that of other animals was fixed by immersion. For perfusion fixation, the anesthetized animals were perfused through the ascending aorta with 1 l of modified physiological solution (0.8% NaCl, 0.8% sucrose and 0.4% glucose), followed by 2 l of 2.5% glutaraldehyde in 0.1 M cacodylate buffer (pH: 7.4). Immersion fixation was performed by dropping the fixative onto the exposed surface of the nasal cavity at the level of the dorsal endoturbinals, in anesthetized animals. Then, the specimens were immersed in the same fixative at room temperature for 2–3 hr. The tissues were stored overnight in buffer with 30% saccharose. After three 5-min washes in buffer, they were postfixed in 1% O_5O_4 in the same buffer, at pH 7.2, for 1 hr. Later, they were washed, dehydrated through an ethanol series, cleared in acetone, and embedded in Araldite. Semithin sections (about 1- μ m-thick) and ultrathin sections (about 0.07- μ m-thick) were cut (Sorvall Porter-Blum ultramicrotome), stained with toluidine blue and double-stained with uranyl acetate and lead citrate, respectively. Ultrathin sections were examined in a Siemens ELMISKOP I or Zeiss M-109 Turbo electron microscopes.

RESULTS

Structural differences could not be observed between the OM of males and females.

Light Microscopy

The OM consists of two layers, a superficial OE and a deep lamina propria. The former shows a pseudostratified epithelium containing three morphologically identified cell layers: SC, ORN, and BC (Fig. 1A and B). In addition, ducts of BG and the apical neck region of acini are often observed within the epithelium (Fig. 1B). Duct cells show flattened nuclei in a thin elongated cytoplasm lining the lumen. The SC form a discrete and conspicuous layer in the outer region of the OE. They are columnar and are extended from the basal membrane to the epithelial surface. Oval-shaped nuclei are seen in their apical extremity (Fig. 1A and B). Two different cell types can be distinguished: type I cells with slightly stained cytoplasm and nuclei, and type II, with deeply stained cytoplasm and nuclei. Both types have apocrine-like protrusions in the luminal surface (Fig. 1B). These protrusions appear as pedunculated or nonpedunculated. The ORN show a typical flask-like shape. The nuclear region is usually situated below the nuclear level of the SC. The cytoplasm appears pale. The rounded nuclei of the ORN show a slightly stained karioplasm with peculiar and enormous bulks of heterochromatin resembling a nucleolus (Fig. 1A and B). Basal cells are confined to the region of the OE adjacent to the basal membrane (Fig. 1A). Two types of cells are found: globose basal cells (GBC) and flat basal cells (FBC). The GBC show pale cytoplasm and nuclei (Fig. 1B). The FBC show their nuclei with the long axis usually parallel to the basal membrane. Both cytoplasm and nuclei are heavily stained (Fig. 1B).

The lamina propria contains unmyelinated olfactory nerves, BG, loose connective tissue with fibroblasts, scarce collagen fibers, blood vessels, and myelinated nerves. Large bundles of unmyelinated olfactory fibers, surrounded by Schwann cells are seen (Fig. 1C).

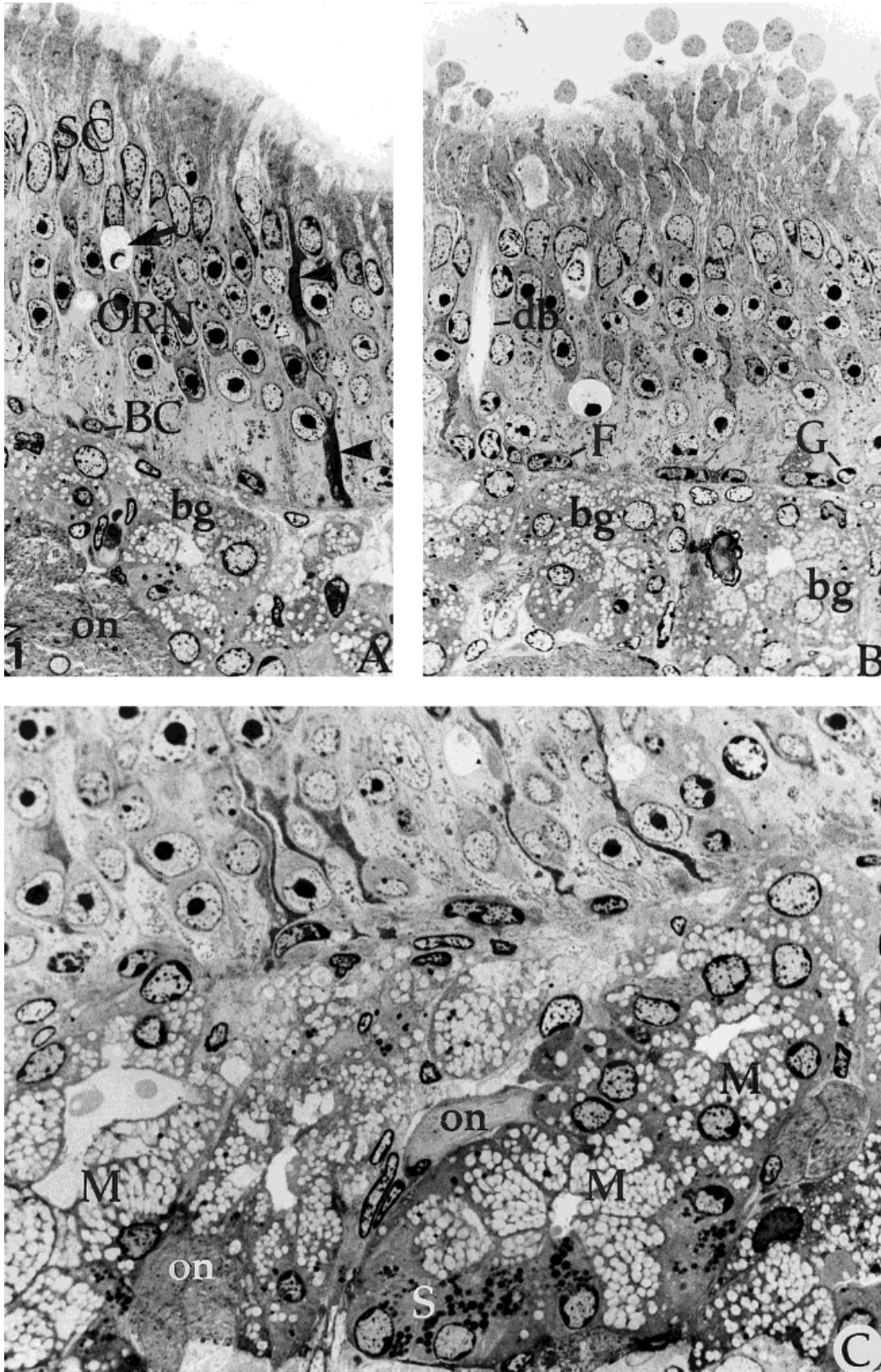


Fig. 1. Photomicrographs of semithin sections of *Chaetophractus villosus* olfactory mucosa. **A:** The olfactory epithelium (OE) contains one row of nuclei of supporting cells (SC), some rows of olfactory receptor neurons (ORN), and one row of basal cells (BC). Processes of type II SC are clearly seen crossing the epithelium (arrowheads). An apoptotic body is seen in the epithelium (arrow). Bowman's glands (bg) and olfactory nerves (on) are visible in the lamina propria. $\times 400$. **B:** Numerous

apocrine-like protrusions of SC are located in the apical surface. The two types of BC: flat basal cell (F) and globose basal cell (G) are distinguished. A duct (db) of Bowman's glands (bg) reaches the epithelial surface. $\times 400$. **C:** Detail of the basal portion of the OE and of the lamina propria. The BG contain mucous (M) and serous (S) cells. on, olfactory nerves. $\times 1,000$.

The BG consist of branched tubulo-acinar endpieces. The latter are separated by a thin layer of connective tissue. The glands are mixed and composed of mucous and serous secretory cells (Fig. 1C). We classify those cells as mucous and serous in terms of their light and electron microscopic appearance (Tandler and Phillips, 1993; Tandler, 1993). Both cell types may be seen in a single endpiece but mucous cells are always more numerous. Both types are pyramidal-shaped with round or oval basal nuclei. The mucous cells contain large, light, closely packed and ill-defined granules. Serous cells have small, discrete, homogeneous and dark granules (Fig. 1C).

Electron Microscopy

Olfactory epithelium. Electron microscopy confirms that the OE is pseudostratified, and that it contains three types of epithelial cells.

Supporting cells. Electron microscopy shows two cell types (type I and type II). Both have peculiar features: apical apocrine-like protrusions, extensive development of smooth endoplasmic reticulum (SER) in their apical portion, apical secretory, and phagosomes. Additionally, some SC contain apoptotic bodies.

Type I. The apical surface shows long microvilli forming a dense network between the olfactory knob and cilia (Fig. 2). Some cells have enormous ovoid or irregularly shaped apocrine-like protrusions of varying length and diameter among the microvilli (Fig. 2). Many apical protrusions are attached to the apical membrane of the SC by a long thin stalk (Fig. 3). Pinching-off appears to be caused by a progressive thinning of the connecting stalk. The protrusions contain widespread tubular SER and mitochondria (Figs. 2 and 3). Abundant SER and mitochondria are seen in the apical cytoplasm (Fig. 2). This dense SER network is similar to that found in the protrusions. The SER is organized in an intricate system of branched and anastomosed tubular membranes. An interesting feature of some SC is represented by scarce membrane-bound secretory granules found in the apical cytoplasm. They have a finely granular and lucent matrix, similar to that found in the mucous cells of the BG (Fig. 4). Scarce rough endoplasmic reticulum (RER), multivesicular bodies, and bundles of intermediate filaments are seen in the cytoplasm (Figs. 5 and 6). The nuclei are oval with a thin rim of chromatin at the periphery. Fine chromatin clumps appear scattered in the nucleus (Fig. 6). Only a few nucleoli were seen. *Zonula occludens* and *zonula adherens* indicate the close relationship between ORN and SC as well as between neighboring SC (Fig. 7). It is noteworthy that *macula adherens* was not seen in junctional complexes. However, *macula adherens* was found between the basolateral mem-

branes of SC and BC. Thin intercellular spaces may occur between SC and ORN in the middle third of the OE. Microvilli project from the evaginated surfaces of bordering cells into the intercellular spaces (Fig. 6). The basal cytoplasm forms basilar expansions, lying on the basal lamina (Fig. 5). They contain SER, mitochondria, and vesicles. Phagosomes are frequently observed in the subnuclear cytoplasm, specially in the basilar expansions. Each phagosome is formed by a single membrane, which encircles partially degraded mitochondria, mielinic figures, and amorphous electron-dense material. (Figs. 8 and 9). Some SC show well-preserved apoptotic bodies engulfed in the cytoplasm (Fig. 9). Those bodies show oval cytoplasmic masses with nuclei. The nucleus has characteristic clumps of chromatin closely opposed to the inner membrane. A pale zone with membrane figures is located between the cytoplasm of the SC and the apoptotic body (Fig. 9). Some SC show rounded pale zones with cell fragments. These zones probably represent a different view of the pale zone surrounding the apoptotic bodies. (Fig. 10).

Type II. The cell body is thinner and more irregularly contoured than that of type I (Fig. 6). Type II is less frequent than type I. The cytoplasm is electron-dense with abundant mitochondria. The nucleus is elongated and more electron-dense than type I. All the other characteristics described in type I are also seen in type II.

Olfactory receptor neuron. The perykaryon is frequently observed in contact with other ORN or with basilar expansions of SC (Fig. 11). A peripheral dendritic process is extended from the cell body towards the epithelial surface (Fig. 11), whereas a central axon traverses the basal lamina. The dendrite protrudes above the epithelial surface forming the olfactory knob (Figs. 2 and 12). Dendrites are easily distinguished from the surrounding SC by their electron-lucent cytoplasm with tubular mitochondria, small vesicles, and longitudinally oriented neurotubules (Figs. 7 and 11). Cilia protrude from the surface of olfactory knobs (Fig. 12A). The internal structure of the cilia is similar to that of ordinary motile cilia. It also shows accessory structures. One of these structures is the striated rootlet fiber, which appears as a striated bundle of filaments (Fig. 12A). Another one is the basal foot, which extends radially from the basal corpuscle (Fig. 12A). Its cross-sections reveal a characteristic pinwheel configuration (Fig. 12B). A prominent Golgi apparatus, generally associated with vesicles and multivesicular bodies, occupies the supranuclear region (Fig. 11). The perinuclear cytoplasm is scanty and shows numerous free ribosomes, RER, and tubular mitochondria. Small vesicles, lipofuscin granules, lysosome-like bodies, neurofilaments, and multi-

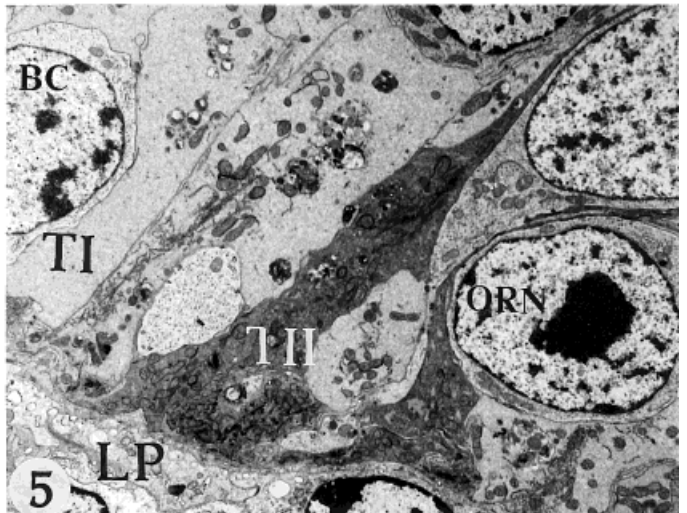
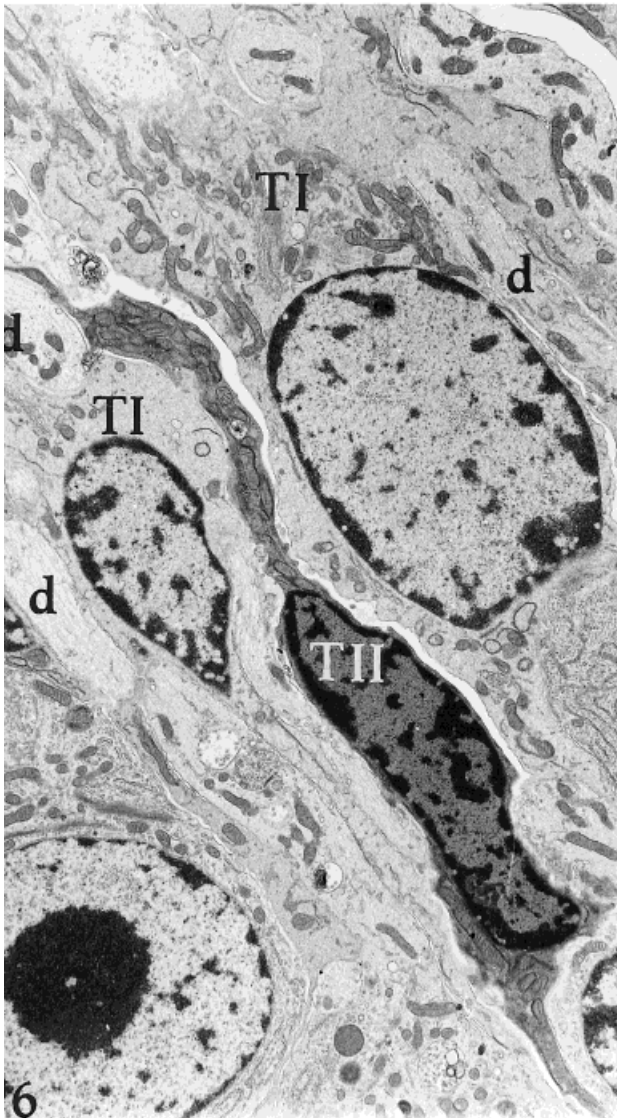
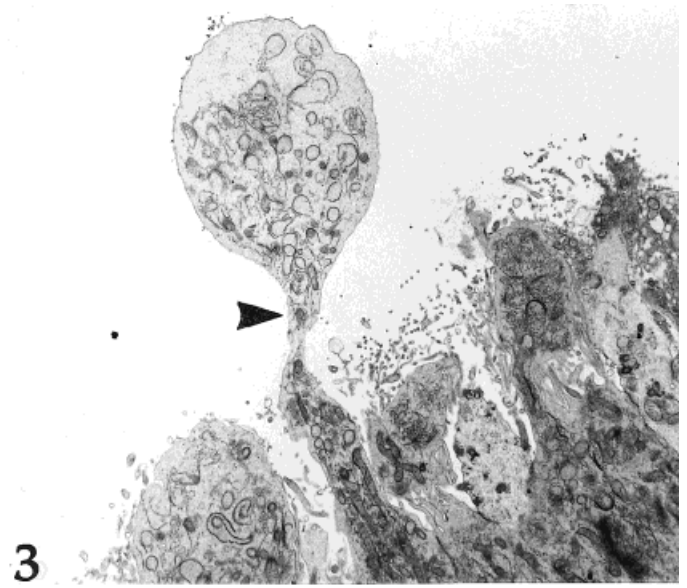
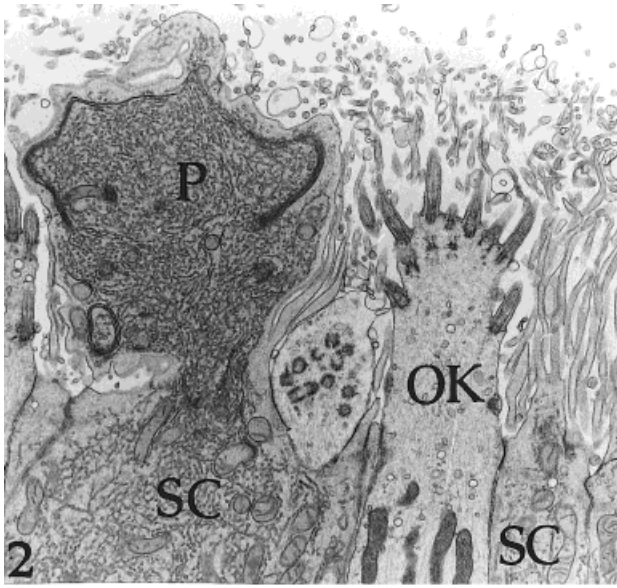
Fig. 2. Electron micrograph of the apical region of the olfactory mucosa. Olfactory knobs (OK) are seen between long microvilli of the supporting cells (SC). Apical protrusions (P) of the SC are filled with a dense network of profusely branched tubular smooth endoplasmic reticulum (SER). $\times 8,000$.

Fig. 3. Apical protrusion of the SC connected to the luminal surface by a thin long stalk (arrowhead). It is filled with a network of tubular SER. $\times 4,800$.

Fig. 4. Apical region of the type I SC. The intricate system of branching and anastomotic tubular membranes of SER are observed. A membrane-bound vacuole containing a lucent matrix (star) is closely associated with the luminal surface. $\times 22,200$.

Fig. 5. Basilar expansions of both types of SC in the basal region of the OE. The pale cytoplasm of type I (TI) cell is intercalated with electron dense cytoplasm of type II (TII). They contact olfactory neurons (ORN) and basal cells (BC). LP, lamina propria. $\times 3,300$.

Fig. 6. Two morphologically distinct types of SC. Type I (TI) has a pale cytoplasm and nucleus. The perinuclear cytoplasm contain tubular mitochondria, SER, rough endoplasmic reticulum (RER), and Golgi complexes. Type II (TII) is thinner and has a more irregular contour. Cytoplasm and nucleus are more electron-dense than in type I. The cytoplasm has abundant mitochondria and SER. Dendritic processes (d) of ORN are frequently seen between the SC. $\times 5,000$.



Figs. 2-6.

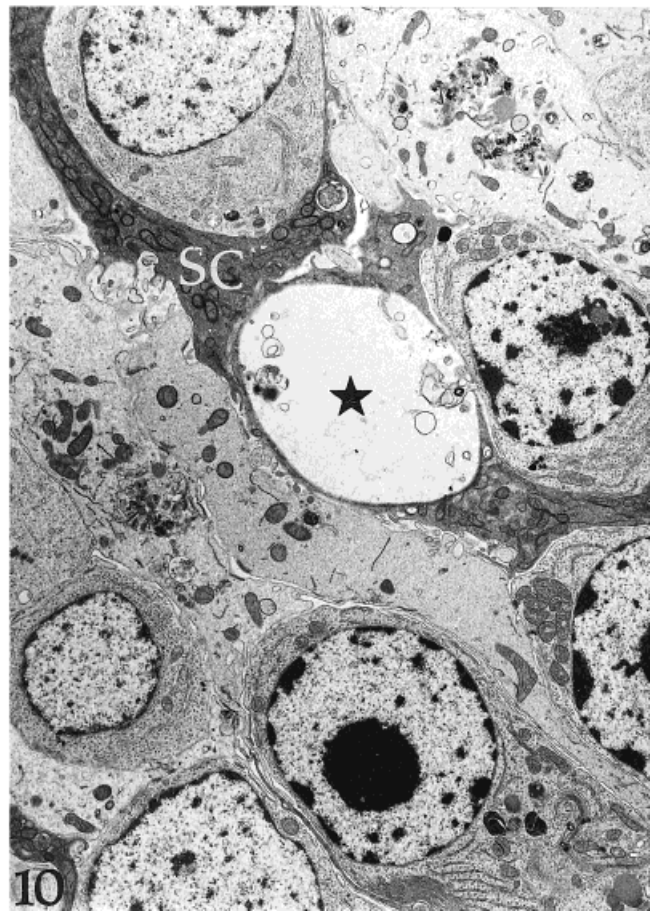
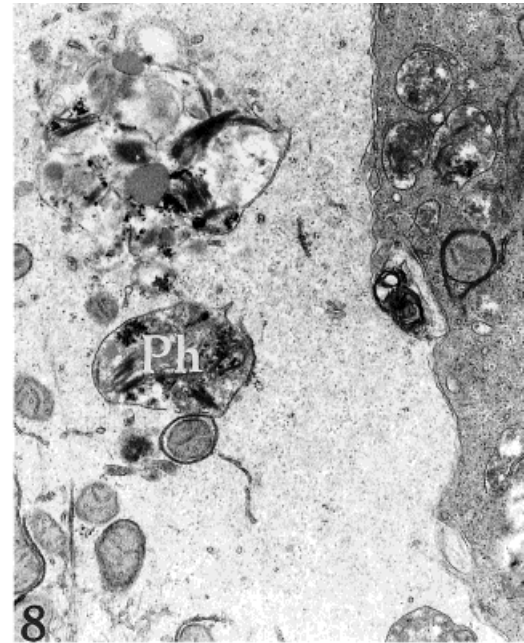
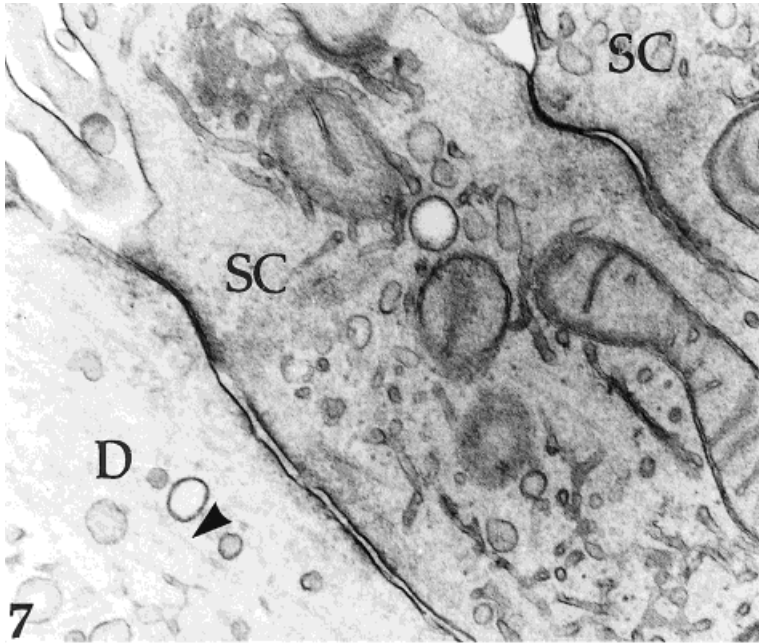


Fig. 7. Detail of the apical surface of the OE. The supporting cell (SC) profiles are characterized by many SER and mitochondria. The apical part of the dendrites (D) show small vesicles and neurotubules (arrowhead). Note the absence of *macula adherens* in the junctional complex between ORN and SC as well as between neighboring SC. $\times 15,000$.

Fig. 8. The infranuclear cytoplasm of Type I (light) and Type II (dark) SC showing many phagosomes (Ph) and mitochondria. $\times 15,000$.

Fig. 9. Well-preserved, large apoptotic body with characteristic nuclear chromatin clumps is seen engulfed by type I supporting cell (SC). Note the pale zone (star) with membrane figures located between the SC and the apoptotic figure. Ph, phagosome. $\times 9,700$.

Fig. 10. Rounded pale zone (star) with membrane figures in type II supporting cell (SC). $\times 4,300$.

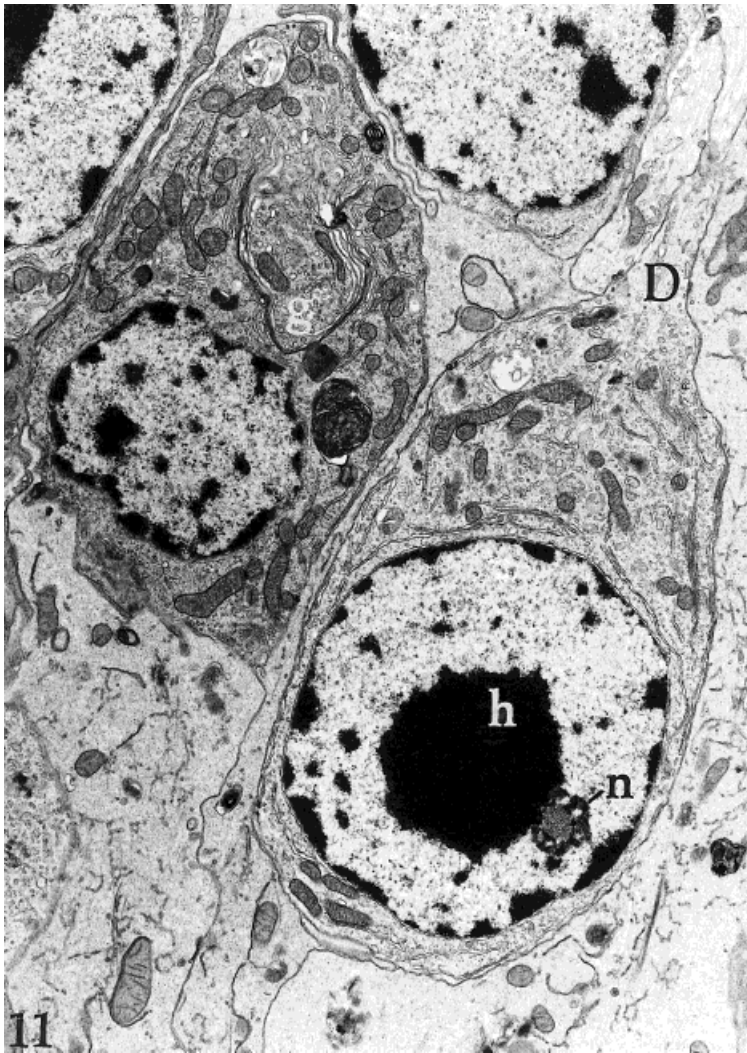
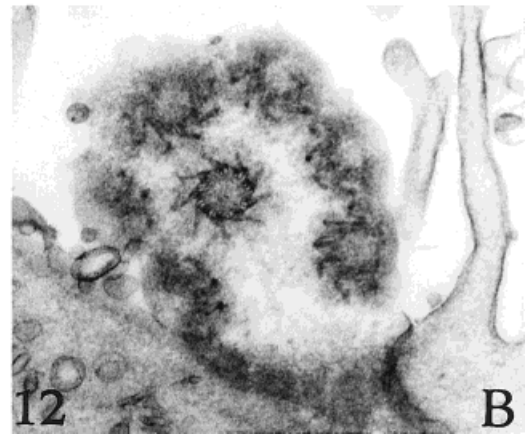
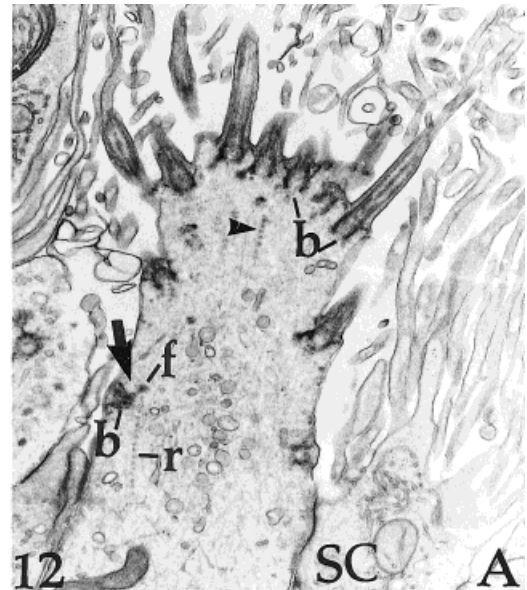


Fig. 11. Longitudinal section including soma of two types of ORN. A neuron with electron-dense cytoplasm and irregularly shaped nucleus is observed at the upper left. A Golgi apparatus (g) associated with vesicles and multivesicular bodies occupies the supranuclear region. The typical neuron with pale cytoplasm shows a dendritic process (D) extended towards the surface. Perinuclear cytoplasm is scanty and numerous free ribosomes, RER, tubular mitochondria, small vesicles, lipofuscin granules, and multivesicular bodies are observed. The nucleus is pale, spherical, and it shows an enormous central heterochromatin clump (h),

vesicular bodies are also seen. The infranuclear cytoplasm exhibits tubular mitochondria, free ribosomes, RER, and scarce SER (Figs. 10 and 11). The nuclei are clearly distinguishable from those of SC. They are spherical and pale, with scanty peripheral chromatin clumps. An enormous central heterochromatin block appears associated with the nucleolus (Fig. 11). Axonal processes are collected before penetrating the basal lamina (Fig. 13B). They form unmyelinated olfactory nerve bundles in the lamina propria. Some neurons show a slightly more electron-dense cytoplasm and an irregular shaped nucleus (Fig. 11).

Basal cells. a) *Flat basal cells.* They are situated above the basement membrane. The cytoplasm and nucleus are slightly electron-dense (Fig. 13A). The nucleus is elon-

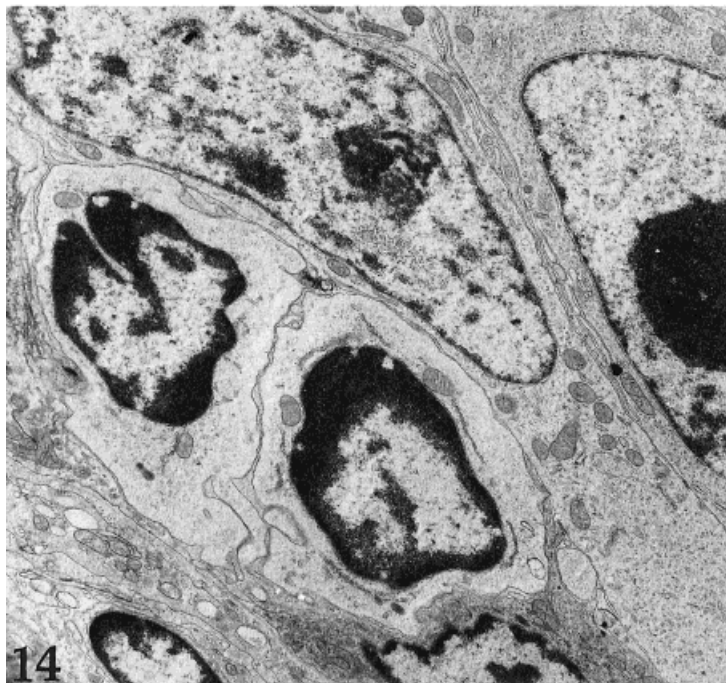
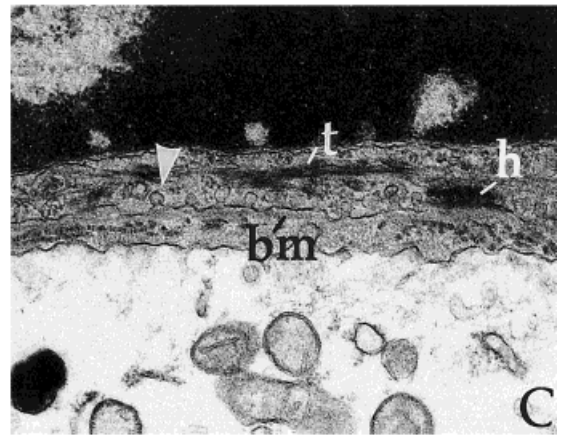
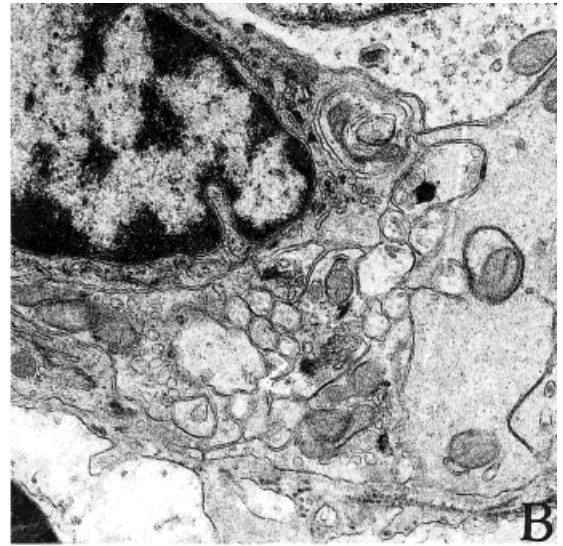
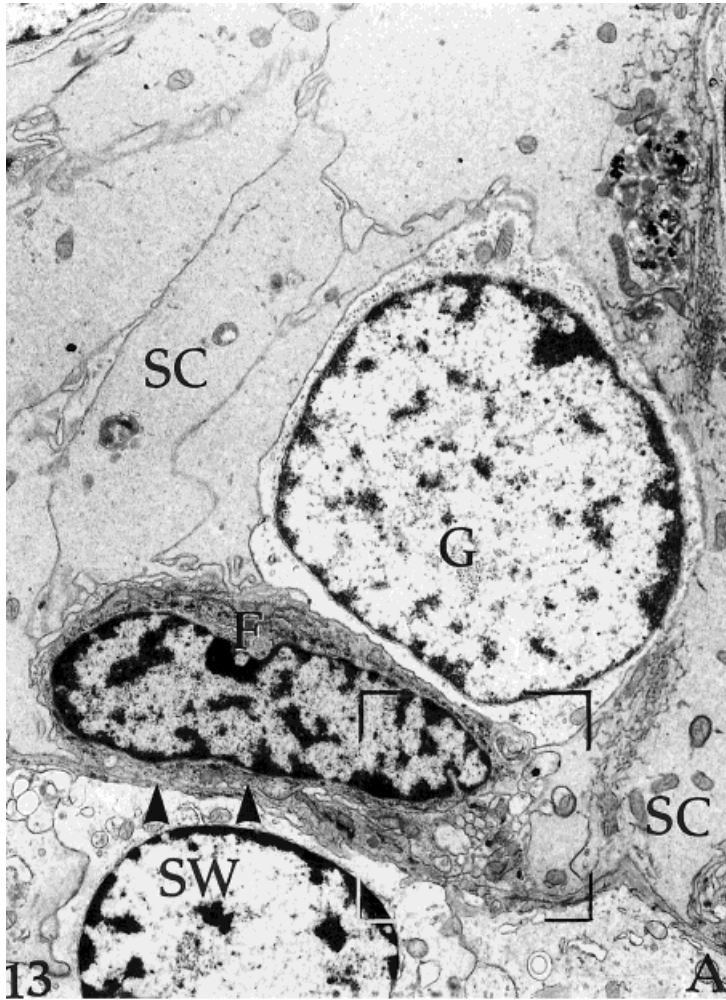


associated with the nucleolus (n). $\times 8,000$.

Fig. 12. **A:** Longitudinal section of the olfactory knob with adjacent supporting cell (SC). This process is ciliated and a number of basal corpuscles (b) are sectioned in different planes. Neurotubules, rootlet fibers (arrowhead), and small vesicles are prominent constituents of the cytoplasm of the distal process. The arrow marks the relationship between the basal foot (f), the basal corpuscle (b), and the rootlet fibers (r). $\times 15,000$. **B:** Cross-section of an olfactory knob showing numerous basal feet. $\times 37,500$.

gated, with the long axis parallel to the basal lamina. It has a dense chromatin pattern and usually one nucleolus. Some nuclei appear indented (Fig. 13B). The cytoplasm is characterized by thin processes that generally ensheath bundles of olfactory axons (Fig. 13B). Interdigitations are seen between these cells and the SC basilar expansions (Fig. 13A). The usual cytoplasmic organelles are: mitochondria, RER, Golgi apparatus, and multivesicular bodies. Conspicuous bundles of tonofilaments, extended across the entire cytoplasm are observed (Fig. 13C). The plasma membrane contacting the basal lamina shows numerous pynocytic vesicles and hemidesmosomes (Fig. 13C).

b) *Globose basal cells.* They are situated above and among the FBC. They have an ovoid or round profile, with



Figs. 13-15.

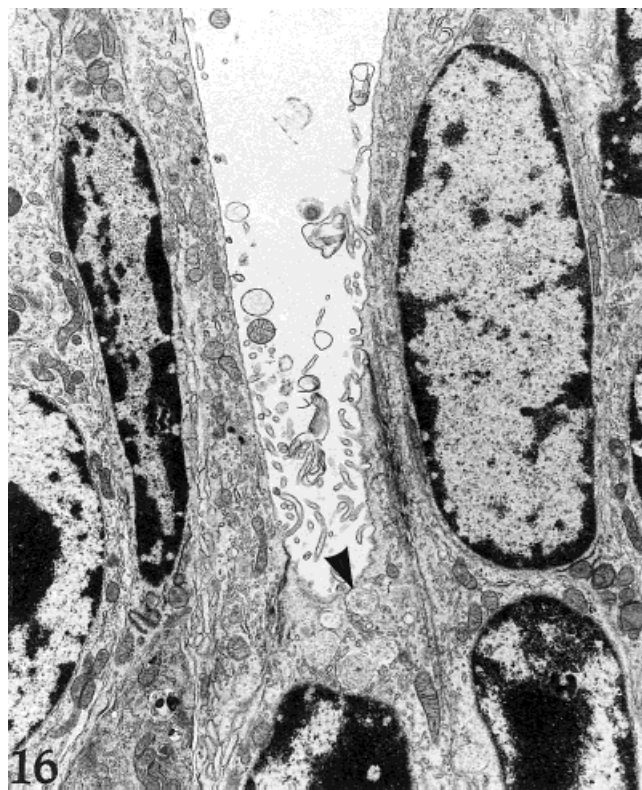
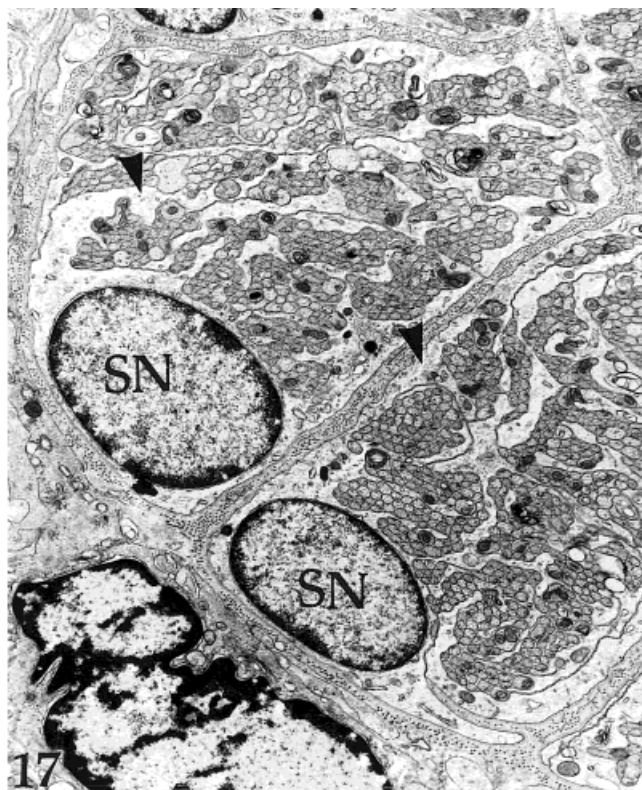


Fig. 16. The duct of the Bowman's gland showing flattened cells with scarce microvilli and secretory granules (arrowhead). $\times 6,400$.

Fig. 17. A restricted region of an olfactory nerve fascicle demonstrating the relation of the Schwann cells with olfactory axons. The axons are



grouped into small fascicles, and the fascicles are in turn unsheathed by mesaxons (arrowheads) of the Schwann cells. SN, Schwann cell nucleus. $\times 6,000$.

a large nucleus and scarce cytoplasm (Fig. 13A). Both nucleus and cytoplasm are electron-lucent. The nucleus is round and pale with clear chromatin. Nucleoli were not frequently seen. The cytoplasm contains numerous free ribosomes, but the other organelles are scarce. It lacks bundles of tonofilaments.

Mitotic figures and apparently newly generated cells are frequently observed in the basal region of the OE (Figs. 14 and 15). These undifferentiated cells show many free ribosomes, few and small organelles, and irregularly shaped nuclei (Figs. 14 and 15).

Ducts of Bowman's glands. Cells lining the ducts have oval nuclei, with the long axis perpendicular to the basal membrane, and a thin cytoplasmic layer. The luminal surface shows short microvilli. There are junctional complexes, without *macula adherens*, between ductal cells. The same complexes are seen between SC and ductal cells. Mitochondria, Golgi apparatus, SER, RER, and bundles of

tonofilaments are seen in the cytoplasm. Secretory granules similar to those found in the mucous cells of the BG are also seen (Fig. 16).

Lamina propria. The lamina propria includes scanty connective tissue, BG, olfactory nerves, and blood vessels.

Olfactory nerves. The olfactory nerves are unsheathed by Schwann cells. The latter exhibit cytoplasmic processes (mesaxons), which branch between the axons separating them into bundles (Fig. 17). Each bundle contains closely packed axons. The axons have neurofilaments, vesicles, and mitochondria. The olfactory Schwann cells show scarce cytoplasm and a round nucleus. They are encircled by a basal lamina and scanty collagen fibers (Fig. 17).

Bowman's glands. The tubulo-acini are composed of two morphologically distinct cell types: the mucous cells (MC) and the serous cells (SR).

Fig. 13. **A:** Basal region of the OE. The flat basal cell (F) contacting the basal lamina is characterized by cytoplasm and nuclei heavily stained. Globose basal cell (G) lies above the flat basal cell (FBC) showing pale cytoplasm and nucleus. The basilar expansions of the supporting cells (SC) are observed between basal cells. SW, Schwann cell. $\times 6,600$. **B:** Higher magnification of the rectangle in A shows the FBC ensheathing olfactory axon fibers. $\times 17,000$. **C:** Higher magnification of a portion of a FBC cell, similar to the area labeled with arrowheads in A. Note the conspicuous bundles of tonofilaments (t). Numerous pynocytic vesicles

(arrowhead) and hemidesmosomes (h) are associated with the plasmatic membrane contacting the basement membrane (bm). $\times 24,000$.

Fig. 14. Two putative undifferentiated cells in the basal region of the OE. They contain many free ribosomes, few and small organelles, and irregularly shaped nuclei. $\times 6,800$.

Fig. 15. Basal region of the OE showing several types of cells. Chromosomes (Cr), ovoid mitochondria, and free ribosomes and SER are seen in a mitotic cell (1). (2) An undifferentiated cell. (3) ORN. $\times 4,800$.

The MC are the most numerous. Their luminal surface is lined with microvilli (Fig. 18). Some MC show a balloon-like protrusion containing SER (Fig. 19). These protrusions are similar to those of SC. Presumably, they may be interpreted as an apocrine-like type of secretion. Laterally, the plasmalemma is joined to that of adjacent cells by a junctional complex composed of *zonula occludens* and *zonula adherens*. *Macula adherens* occurs close to the junctional complex but it is not constantly observed in all sections. The basally situated nucleus is large, round, and euchromatic (Fig. 18). Electron-lucent secretory granules fill the entire cytoplasm. These structures are bound by a single membrane. They contain two distinct finely granular materials. One appears with low electron density. The other is more electron-dense and heterogeneous (Fig. 18). In some granules, punctate densities occur (Fig. 18). The mode of discharge of secretory granules may be described as a merocrine process (Fig. 20). The MC are characterized by an extraordinarily well-developed tubular SER (Figs. 19 and 21). The SER tubules are randomly oriented and closely packed, like those of SC. A few cisterns of RER in continuity with the SER can be observed. Dilated cisterns of endoplasmic reticulum with a moderately dense flocculent material are often found. Sometimes, the dilated cisterns attain the size of mature secretory granules (Fig. 22). The Golgi apparatus is mainly seen in apical and middle cytoplasmic regions associated with putative immature secretory granules (Fig. 21).

The SR show numerous electron-dense granules. Their large and basally situated nuclei are oval or round. The luminal surface is lined with microvilli (Fig. 23). Junctional complexes, with *zonula occludens*, *zonula adherens*, and *macula adherens*, join neighbor cells (Fig. 23). These cells have all the structural hallmarks of cells geared for synthesis of proteins for export. The cytoplasm contains scattered mitochondria, an extensive supranuclear Golgi apparatus with small vesicles and condensed vacuoles (Fig. 24). The infranuclear region has a great whirly tightly packed set of RER cisterns (Fig. 23). Secretory granules are usually less abundant and more separated than those of MC. However, they occupy the supranuclear region. They are round or oval and membrane-bound. They showed varying degrees of electron density from cell to cell and sometimes within the same cell (Fig. 23). These differences may reflect different stages of the secretory cycle and the degree of maturity of individual serous granules. Their number varies from cell to cell. Some cells have numerous granules almost filling the apical cytoplasm. Other cells contain only a few granules. Indeed, SR without granules is frequently observed. We did not observe images providing clues to the secretory mechanisms. The basal surface of acinar cells directly contact the basement membrane. Mitotic figures, intercellular canaliculi or myoepithelial cells were not observed in the BG.

Connective tissue. It is scanty and shows fibroblasts, collagen fibers, mast cells, plasma cells, and blood vessels. The plasma cells are intimately related with the basal

region of the BG (Fig. 25). A rich vascular supply with many nonfenestrated capillaries (Fig. 26), and venous sinuses are observed in the interstitial areas of the lamina propria.

DISCUSSION

The OM of the armadillo *Chaetophractus villosus* is organized according to the typical plan of most vertebrates. The ORN and the BC have morphological features similar to the corresponding cells of the OM from other species (Graziadei, 1973; Farbman, 1992).

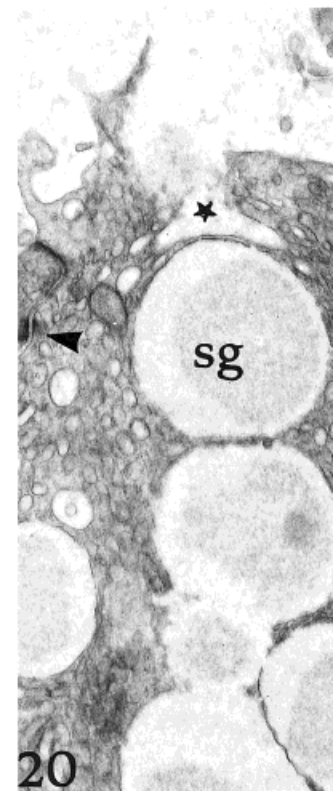
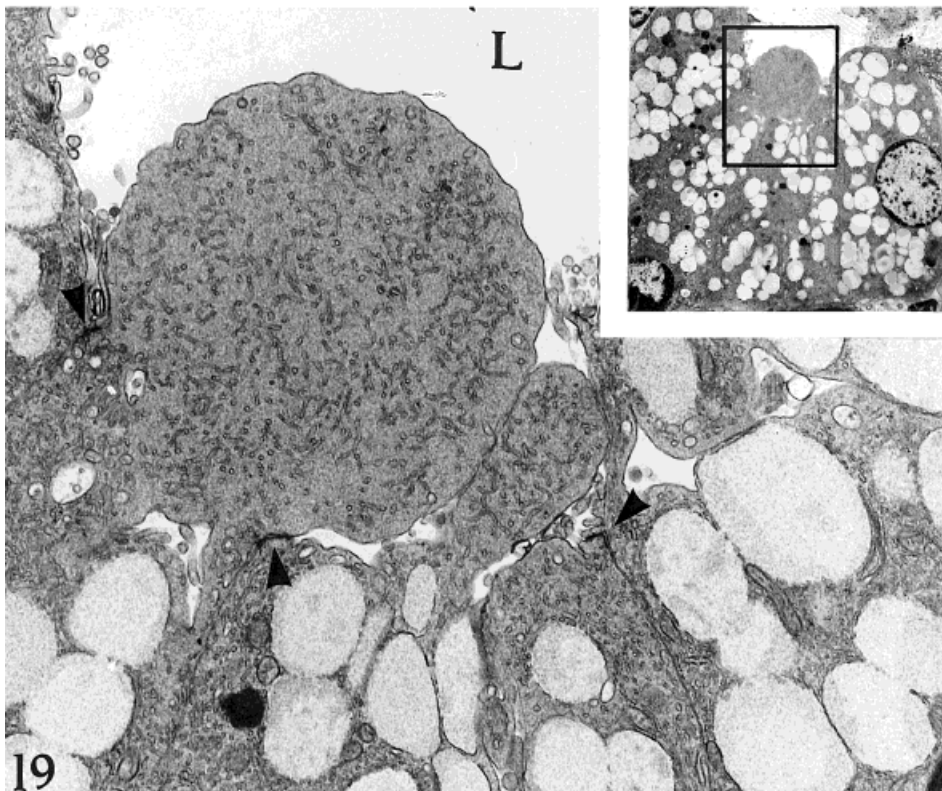
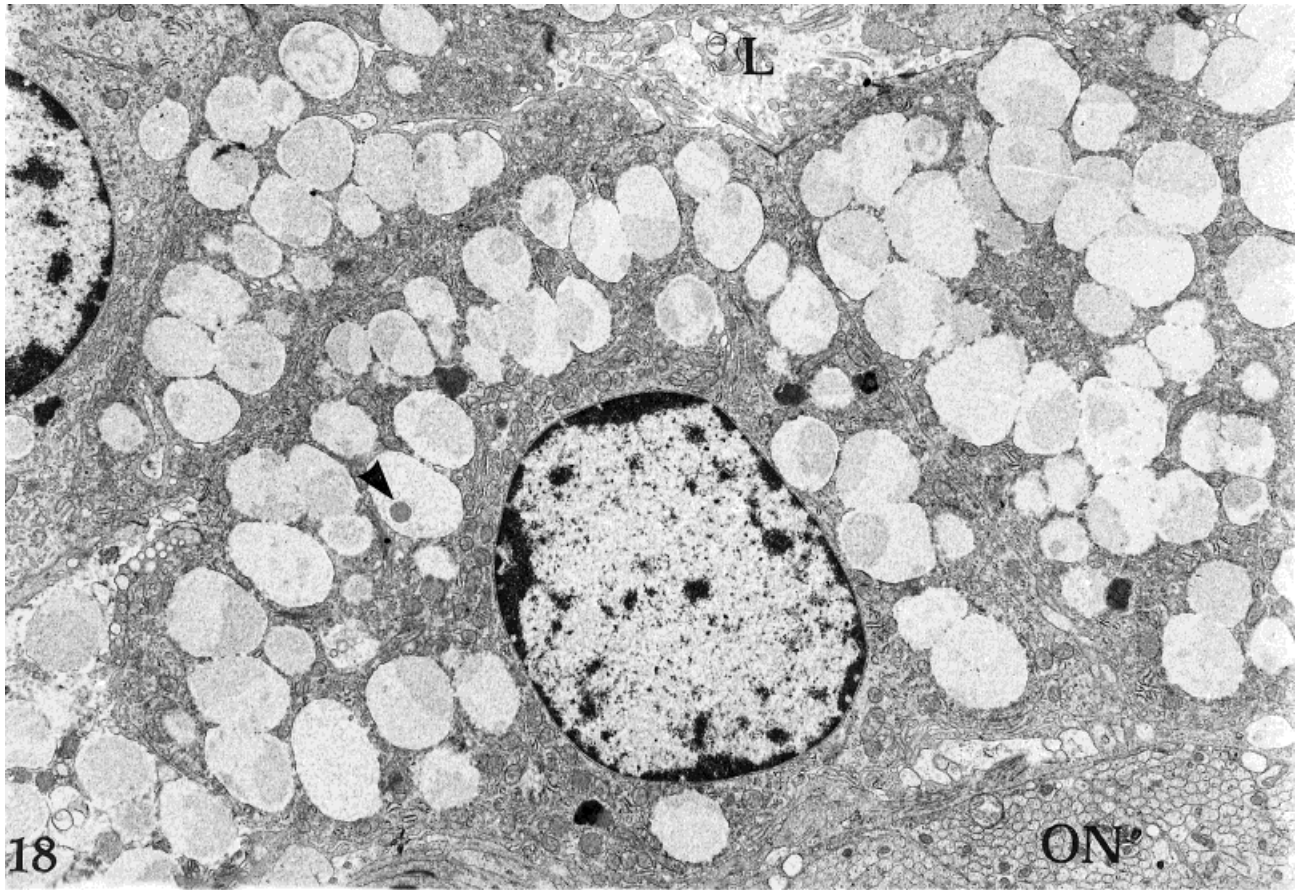
The SC of armadillos show peculiar characteristics differentiating them from those found in others mammals. One interesting feature is the presence of secretory granules in their apical portion. As a general rule, the SC of fish, amphibians, reptiles, and birds are specialized for secretion, whereas those of mammals appear to be nonsecretory (Getchell and Getchell, 1992). The only exception was reported by Frisch (1967) in the mouse SC. Armadillos therefore share this property with mice. Another feature of SC is the extensive development of SER. Abundance of SER was also found in sheep, mole, bandicoot, rabbits, guinea pigs, and some primates (Frisch, 1967; Kratzing, 1970; Getchell and Getchell, 1992). On the other hand, abundant SER has been reported in nonciliated, nonsecretory cells of the respiratory epithelium (Martineau-Doiz and Caya, 1996). Abundance of SER in other cellular systems has been associated with several functions (Ponzio, 1996): lipid synthesis, steroid synthesis, glucose metabolism, and detoxification. Lipid synthesis in adipocytes and some glands is suggested by the presence of intracytoplasmic lipid droplets (Bell, 1974; Atoji et al., 1989; Payne, 1994). Cells with high production of steroids generally show mitochondria with tubular cisterns and cholesterol storage (Russell, 1996). Glucose metabolism is related with intracellular glycogen particles (Ponzio, 1996). It is worth noting that none of those features can be assigned to SC. However, SC display an enormous SER. Therefore, the question regarding the functional meaning of that unusual development is posed. In this respect, a paper from Ghadially (1988) might provide a probable explanation. Hypertrophy of liver SER is considered, in that paper, as an adaptive response by which animals metabolize and tolerate xenobiotics at quantities that otherwise would be fatal. According to this opinion, SER would be the seat of enzymes involved in xenobiotic metabolism. In view of these data, we hypothesize that the great development of SER in apical location is related to nasal xenobiotic metabolism. The well-known ability of nasal tissue to metabolize xenobiotic substrates (Lewis and Dahl, 1995) adds support to this hypothesis. Armadillos are powerful diggers, their noses being permanently exposed to a variety of soil materials. In order to counterbalance a probable noxious effect, they are endowed with protective structures situated at the entrance of the nostrils (Affanni et al., 1987). Xenobiotic functions of SC might represent an additional protective function through disposal of foreign

Fig. 18. Survey electron micrograph of a mucous cell of BG. The heterogeneous secretory granules appear composed of materials with two different electron densities. Some granules also contain punctate densities (arrowhead). Additionally these cells contain highly developed SER. L, lumen; ON, olfactory nerve. $\times 6,200$.

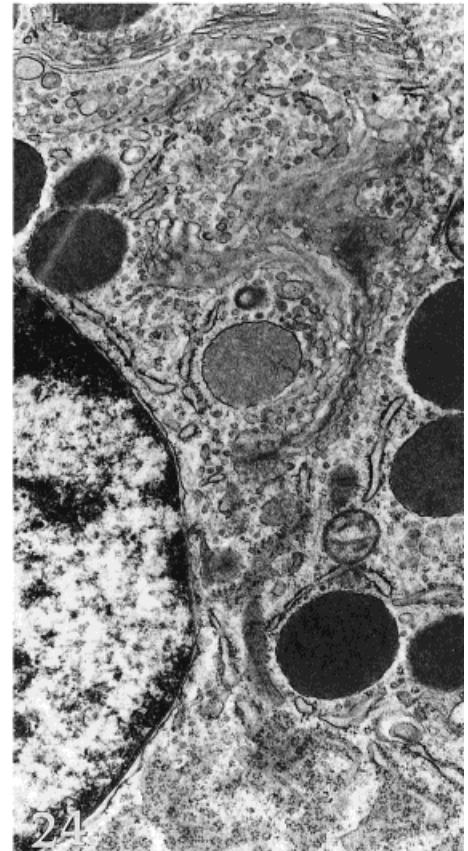
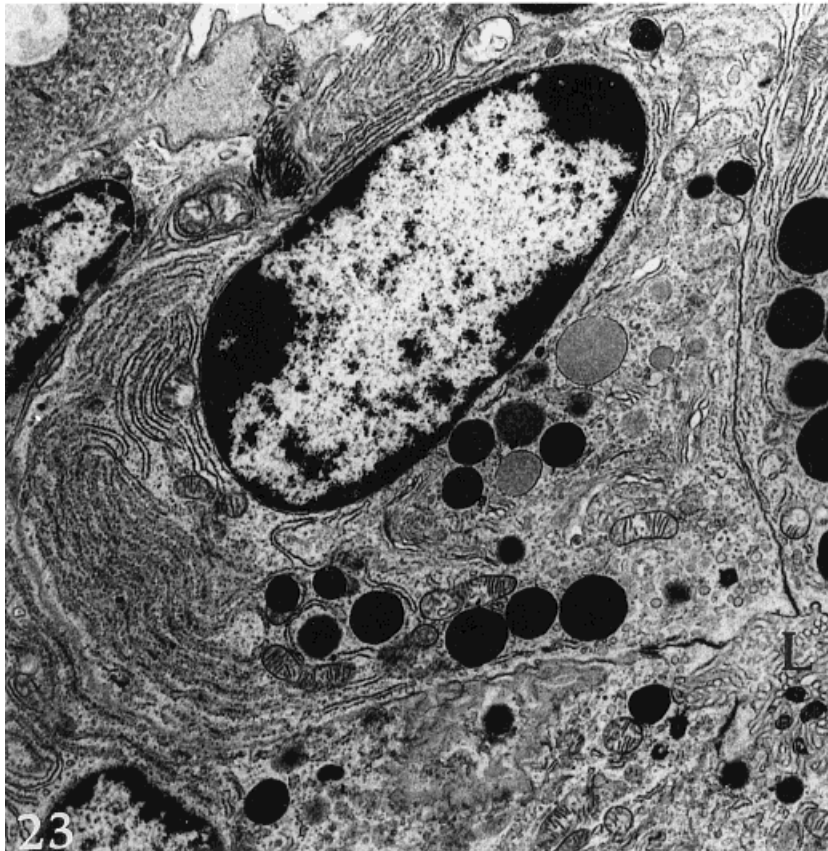
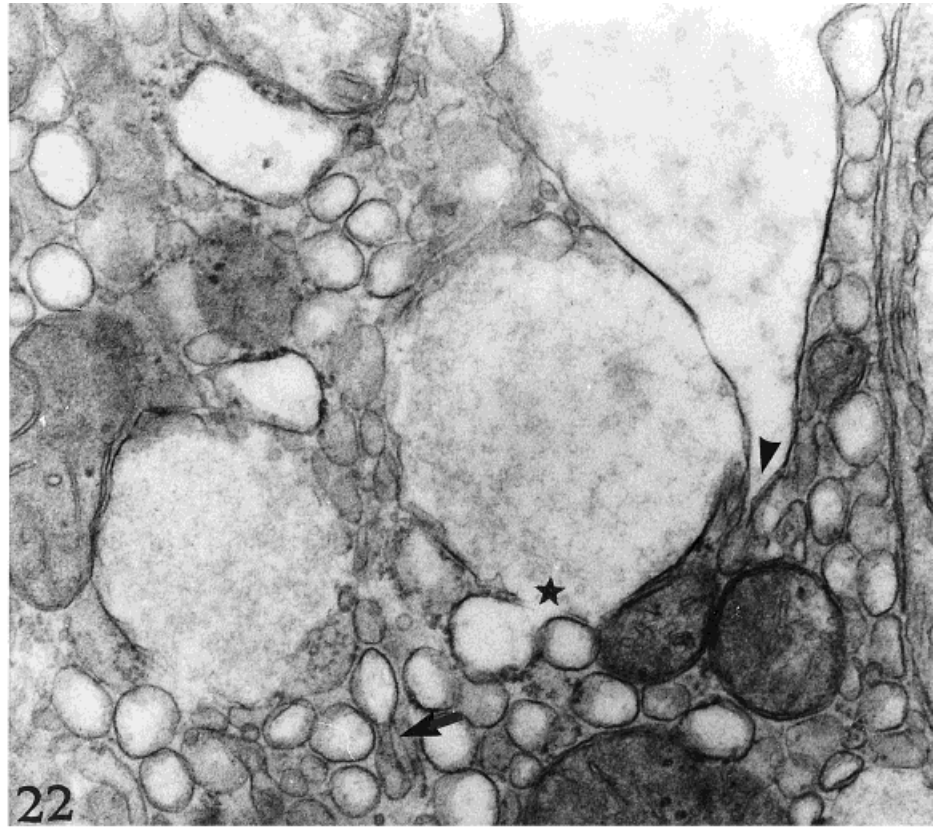
Fig. 19. Higher magnification of the rectangle marked in the inset.

Fig. 20. The secretory granule (sg) appears to be secreted from the cells by a merocrine mechanism (star). The junctional complex shows macula adherens (arrowhead). $\times 15,300$.

Fig. 21. Higher magnification of the rectangle marked in the inset.



Figs. 18-20.



Figs. 21-24.



Fig. 25. A typical plasma cell with dilated cisterns of RER intimately associated with mucous acinar cell (M). $\times 7,000$.

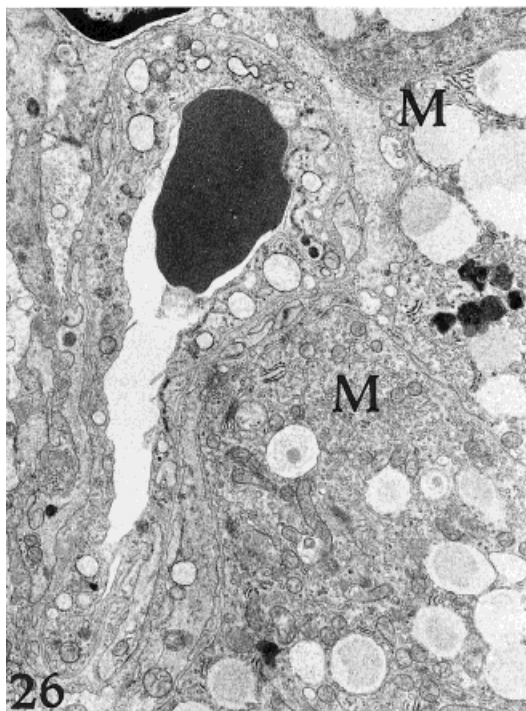


Fig. 26. A nonfenestrated capillary related with mucous acinar cells (M). $\times 7,100$.

Fig. 21. Golgi complex of mucous cells. Note the proximity of the Golgi complex to apparently newly generated secretory granules. $\times 19,700$.

Fig. 22. Higher magnification of a portion of mucous cell. Highly dilated cisterns of endoplasmic reticulum with a moderately dense flocculent material. Highly dilated cistern of SER (arrowhead) in continuity with a nondilated cistern. Dilated cistern of RER coalescing with a highly dilated cistern of SER (star). A tubular cistern of SER with a dilated

materials. Another interesting feature is that in normal adult armadillos, both types of SC show phagosomes and apoptotic bodies in the infranuclear cytoplasmic process. The phagosomes, apoptotic bodies, and cell fragments are probably ORN or SC in various stages of degradation. Phagocytosis of neuronal material by SC was reported only in the chronic period following bulbectomy in adult mice (Suzuki et al., 1995). Phagocytic activity was detected 1 day after bulbectomy in newborn mice (Suzuki et al., 1996). However, during early postnatal development, the OM of animals not submitted to bulbectomy shows phagocytic functions (Suzuki et al., 1995, 1996). Our observation of frequent apoptotic bodies in the SC of normal adult armadillos differs from the above-mentioned reports. As far as we know, our report is the first one indicating the occurrence of SC containing apoptotic bodies in adult normal mammals. This represents a further confirmation of SC phagocytic functions. Magrassi and Graziadei (1995) reported the occurrence of dense bodies representing the terminal phase of apoptotic neurons in the intercellular space of the OM. Our observation of many mitotic figures and undifferentiated cells in the basal layer of the armadillo might presumably be correlated with the numerous apoptotic bodies observed. In fact, studies in adrenal glands suggested that over time, the rate of apoptotic cell loss equals that of cell gain through mitosis (Wyllie et al., 1980). Therefore, the armadillo appears as a convenient model for studying cell death and proliferation in the OE. A detailed knowledge of what induces cell death and disposal of dead cells may provide clues for understanding the control of cell proliferation.

Regarding the presence of two types of SC, light and dark cells have been described frequently in many tissues (López et al., 1992). In the OM, Graziadei and Monti-Graziadei (1979) described light and dark neurons. However, there is still controversy regarding the interpretation of this phenomenon. Some authors interpret their appearance as an artifact caused by trauma involved in processing the tissue (Sinowatz and Amselgruber, 1986). Other authors propose that light and dark cells may reflect different degrees of cell activity (López et al., 1992). The assumption of an artifact due purely to tissue processing is unlikely because light and dark SC are closely apposed. The presence of SER, phagosomes, apoptotic bodies, apocrine-like protrusions was observed in both cell types of the armadillo. These observations suggest the possibility of light and dark SC could be related with different metabolic activities.

Another interesting fact of this study is the occurrence of apocrine-like protrusions in SC. The apocrine release of apical protrusions or contents is carried out by three distinct processes: decapitation, pinching off, and breakdown of the plasma membrane that covers them (Gesase et al., 1996). This study has demonstrated the presence of apical blebs and their decapitation. Apocrine secretion has

extremity is shown (arrow). $\times 40,500$.

Fig. 23. Survey electron micrograph of a serous cell of BG. The cytoplasm shows numerous secretory granules, some of which vary in electron density. The great development of the RER forming a whorl is observed in the basal region. L, lumen. $\times 3,700$.

Fig. 24. Immature serous secretory granule associated with the Golgi complex. $\times 16,600$.

been described in amphibian SC (Getchell and Getchell, 1992). On the other hand, the presence of club-like and balloon-like protrusions has been reported in turtles (Wang and Halpern, 1980), snakes (Graziadei, 1973), vulture (Graziadei, 1973), mole (Meinel and Erhardt, 1978), and humans (Polyzonis et al., 1979). Those structures have also been found in the female preovulatory *Rhesus* monkey, probably suggesting an influence exerted by the sexual cycle (Saini and Breipohl, 1976). None of those authors considered the possibility of apocrine secretion. One might speculate that this fact resembles the phenomenon described in retinal rods. The outer segment of the latter cells has been shown to be continually renewed by the repeated lamellar apposition of membranous discs at the base of the outer segments (Young, 1967). In the case of SC, we might wonder if there is a continuous renewal of SER indicating a partial cellular renewal.

The functional role of SC has not yet been extensively analyzed. Some authors, based on the resemblance with glial cells of the central nervous system (CNS), suggest a role similar to that of those cells (Rafols and Getchell, 1983). They are thought to participate in the regulation of the ionic composition of the mucus layer (Getchell et al., 1984), detoxification (Lewis and Dahl, 1995), mucus secretion, molecular transport, and guiding task for developing neurons and their processes (Morrison and Constanzo, 1992). Other roles for SC, if any, remain to be discovered.

Neurons with electron-dense cytoplasm, swollen Golgi and RER profiles, together with increased number of lipofuscin granules, were described as aging elements (Graziadei and Monti Graziadei, 1979). However, in the armadillo, the electron-dense neuronal cytoplasm apparently does not show degenerative organelles. Therefore, we are not prone to consider them as degenerative cells.

Duct cells of BG show secretory activity similar to that described in mice, dogs, and rabbits (Getchell and Getchell, 1992). The ductal cells and the SC of the armadillo have similar ultrastructural characteristics. Similarities between these two cells types were described (Pixley et al., 1997).

The general structure of the BG of the armadillo coincides with reports from other mammals in which there are serous and mucous cells (Getchell and Getchell, 1992). The secretory mechanisms have not been systematically studied at the ultrastructural level. The apparent occurrence of merocrine secretion was demonstrated in bullfrogs (Getchell and Getchell, 1992). The demonstration of merocrine secretion appears to be the first report regarding this point in mammals. Apocrine secretion was reported in mucous cells of rabbits and in human serous cells (Yamamoto, 1976; Lucheroni et al., 1986). Our observation of balloon-like protrusions in mucous cells presumably indicates apocrine secretion. The protrusions display ultrastructural features similar to those of SC. In fact, a common origin and similar antigenic expression patterns of SC and BG has been demonstrated (Schwob et al., 1994; Pixley et al. 1997).

We assign special interest to the finding of plasma cells intimately associated with BG. The secretory component and J chain have been localized in acinar and duct cells of human BG (Mellert et al., 1992). On the other hand, nasal secretion is known to contain immunoglobulins including immunoglobulin A and immunoglobulin M (Kaliner, 1991; Getchell and Getchell, 1991). Therefore, the BG would

represent a site of immune-secretion towards the mucous layer.

Studies on the BG have been less intense than the ones on the OM. However, BG play an important functional role in immunological processes (Kaliner, 1991): xenobiotic activity (Lewis and Dahl, 1995); mucous secretion (Farbman, 1992; Getchell and Getchell, 1992); production of odor-binding proteins and growth factors (Dear et al., 1991; Farbman and Buchholz, 1996), as well as regeneration of the OM (Schwob et al., 1995; Evans et al., 1995; Taniguchi et al., 1996).

We think that our results may help as a basis for further research on the varied phenomena occurring at the level of the OM.

ACKNOWLEDGMENTS

We express our gratitude to Mrs. Isabel Farias and Gabriel Rosa for their technical assistance in electron microscopy. We thank to Dr. Pecci Saavedra and the LANAIS-MIE (School of Medicine, UBA).

LITERATURE CITED

- Affanni JM, Garcia Samartino L. Comparative study of electrophysiological phenomena in the olfactory bulb of some South American marsupials and edentates. In: Bolis L, Keynes RD, Madrell SHP, eds. *Comparative Physiology of Sensory Systems*. London: Cambridge University Press, 1984: 315–331.
- Affanni JM, Garcia Samartino L, Casanave EB, Dezi R. Absence of apnea in armadillos covered by soil. *Resp. Physiol.* 1987;67:239–243.
- Allison AC. The morphology of the olfactory system in the vertebrates. *Biol. Rev.* 1953; 28:195–244.
- Atoji Y, Sugimura M, Suzuki Y. Sebaceous glands of the infraorbital gland of the Japanese serow *Capricornis crispus*. *J. Submicrosc. Cytol. Pathol.*, 1989;21:375–383.
- Baker H. Transport phenomena within the olfactory system. In: Doty RL, ed. *Handbook of Olfaction and Gustation*. New York: Marcel Dekker, Inc., 1995: 173–190.
- Bell M. A comparative study of the ultrastructural of the sebaceous glands of man and other primates. *J. Invest. Dermatol.* 1974;6:132–143.
- Benitez I, Aldana Marcos HJ, Affanni JM. The encephalon of *Chaetophractus villosus*. A general view of its most salient features. *Comunicaciones Biológicas* 1994;12:57–73.
- Dahl AR, Hadley WM. Nasal cavity enzymes involved in xenobiotic metabolism: Effects on the toxicity of inhalants. *Crit. Rev. Toxicol.* 1991;21:345–372.
- Dear TN, Boehm T, Keverne EB, Rabbitts TH. Novel genes for potential ligands-binding proteins in subregions of the olfactory mucosa. *EMBO J.* 1991;10:2810–2819.
- Eisenberg JF. *The Mammalian Radiations. An Analysis of Trends in Evolution, Adaptation, and Behavior*. Chicago: The University of Chicago Press, 1981: 3–56.
- Engelman G. The phylogeny of the Xenarthra. In: Montgomery GG, ed. *The Ecology and Evolution of Armadillos, Sloths and Vermilinguas*. Washington D.C.: Smithsonian Institution Press, 1985: 51–64.
- Evans JE, Miller ML, Andringa A, Hastings L. Behavioral, histological, and neurochemical effects of nickel (II) on the rat olfactory system. *Toxicol. Appl. Pharmacol.* 1995;103:209–220.
- Farbman AI. *Cell Biology of Olfaction*. London: Cambridge University Press, 1992: pp 282.
- Farbman, AI, Buchholz JA. Transforming growth factor α and other growth factors stimulate cell division in olfactory epithelium *in vitro*. *J. Neurobiol.* 1996;30:267–280.
- Ferrari CC. The olfactory structure of the armadillos *Chaetophractus villosus* and *Dasypus hybridus*. Doctoral Dissertation. Buenos Aires University, Buenos Aires, Argentina, 1997.
- Ferreira-Moyano H, Cinelli AR. Axonal projections and conduction properties of olfactory peduncle neurons in the armadillo (*Chaetophractus vellerosus*). *Exp. Brain Res.* 1986; 64:527–534.
- Frisch D. Ultrastructure of mouse olfactory mucosa. *Am. J. Anat.* 1967;121:87–120.

- Gasase AP, Satoh Y, Ono K. Secretagogue-induced apocrine secretion in the Harderian gland of the rat. *Cell Tissue Res.* 1996;285:501–507.
- Getchell ML, Getchell TV. Immunohistochemical localization of components of the immune barrier in the olfactory mucosa of salamanders and rats. *Anat. Rec.* 1991;231:358–374.
- Getchell ML, Getchell TV. Fine structural aspects of secretions and extrinsic innervation of the olfactory mucosa. *Microsc. Res. Tech.* 1992;23:111–127.
- Getchell ML, Rafols JA, Getchell TV. Histological and histochemical studies of the secretory components of the salamander olfactory mucosa: Effects of isoproterenol and olfactory nerve section. *Anat. Rec.* 1984;208:553–565.
- Ghadially FN. Nucleus. In: *Ultrastructural Pathology of the Cell and Matrix*, Vol. 1. 3rd. ed. London: Butterworth, 1988: 104–105.
- Grassé P. Organe olfactif. In: *Traité de Zoologie*, Tomo XII, Masson et C^{ie} eds. Paris: Libraires de L'Académie de Médecine. 1955: 522–552.
- Graziadei PP. The ultrastructure of vertebrates olfactory mucosa. In: Friedmann I, ed. *The Ultrastructure of Sensory Organs*. New York: North-Holland Publishing Co. 1973: 269–305.
- Graziadei PP, Monti Graziadei GA. Neurogenesis and neuron regeneration in the olfactory system of mammals. I. Morphological aspects of differentiation and structural organization of the olfactory neurons. *J. Neurocytol.* 1979;8:1–18.
- Kaliner MA. Human nasal respiratory secretions and host defense. *Am. Rev. Resp. Dis.* 1991; 144:552–556.
- Kratzing JE. The olfactory mucosa of the sheep. *Aust. J. Biol. Sci.* 1970;23:447–458.
- Lewis JL, Dahl AR. Olfactory mucosa: Composition, enzymatic localization and metabolism. In: Doty RL, ed. *Handbook of Olfaction and Gustation*. New York: Marcel Dekker, Inc., 1995: 33–52.
- López JM, Tolivia J, Alvarez-Uria M. Postnatal development of the Harderian gland in the Syrian golden hamster (*Mesocricetus auratus*): A light and electron microscopy study. *Anat. Rec.* 1992;233:597–616.
- Lucheroni A, Maurizi M, Spreca A, Palmerini CA, Binazzi M. Some aspects of the secretory activity of the human olfactory glands. *Rhinology* 1986;24:57–60.
- Magrassi L, Graziadei PPC. Cell death in the olfactory epithelium. *Anat. Embryol.* 1995; 192:77–87.
- Martineau-Doiz B, Caya I. Ultrastructural characterization of the nasal respiratory epithelium in the piglet. *Anat. Rec.* 1996;246:169–175.
- Mc Kenna MC. Toward a phylogenetic classification of the Mammalian. In: Lockett WP and Szalay FS, eds. *Phylogeny of Primates*. New York: Plenum Press, 1975: 21–46.
- Meinel W, Erhardt H. Apical protuberances of supporting cells in the region olfactoria of the mole, *Talpa europaea*, Linnaeus, 1758 (Insectivora, Talpidae). *Cell Tissue Res.* 1978; 193:175–178.
- Mellert TK, Getchell ML, Sparks L, Getchell TV. Characterization of the immune barrier in human olfactory mucosa. *Otolaryngol. Head Neck Surg.* 1992;106:181–188.
- Morrison EE, Costanzo RM. Morphology of olfactory epithelium in humans and other vertebrates. *Microsc. Res. Tech.* 1992;23:49–61.
- Morrison EE, Moran DT. Anatomy and ultrastructure of the human olfactory neuroepithelium. In: Doty R, ed. *Handbook of Olfaction and Gustation*. New York: Marcel Dekker Inc., 1995: 75–97.
- Novacek MJ. The radiation of placental mammals. In: D. Prothero, R. Schoch and R. Spencer (eds.) *Randall Spencer Series, ed. Major Features of Vertebrate Evolution. Short Courses in Paleontology*. Number 7. London: A Publication of the Paleontological Society, 1994: 220–237.
- Payne AP. The Harderian gland: A tercentennial review. *J. Anat.* 1994;185:1–49.
- Pixley SK, Farbman AI, Menco BM. Monoclonal antibody marker for olfactory sustentacular cell microvilli. *Anat. Rec.* 1997;248:307–321.
- Polyzonis BM, Kafandaris PM, Gigis PI, Demetriou T. An electron microscopic study of human olfactory mucosa. *J. Anat.* 1979;128: 77–83.
- Ponzio R. Sistema de endomembranas. In: *Biología Celular y Molecular*, P De Robertis ED (h), Hib J, Ponzio R, eds. Buenos Aires: El Ateneo, 1996: 221–273.
- Rafols JA, Getchell TV. Morphological relations between the receptors neurons, sustentacular cells and Schwann cells in the olfactory mucosa of the salamander. *Anat. Rec.* 1983; 206:87–101.
- Russell LD. Leydig cell structure. In: Payne AH, Hardy MP, Russell LD, eds. *The Leydig Cell*. Vienna: Cache River Press, 1996: 43–96.
- Saini KD, Breipohl W. Surface morphology in the olfactory epithelium of normal male and female Rhesus monkeys. *Am. J. Anat.* 1976;147: 433–436.
- Schwob JE, Huard JMT, Luskin MB, Youngtob SL. Retroviral lineage studies of the rat olfactory epithelium. *Chem. Senses* 1994;19:671–682.
- Schwob JE, Youngtob ST, Mezza RC. Reconstitution of the rat olfactory epithelium after methyl bromide-induced lesion. *J. Comp. Neurol.* 1995;359:15–37.
- Sinowatz F, Amselgruber W. Postnatal development of the bovine Sertoli cells. *Anat. Embryol.* 1986;174:413–423.
- Suzuki Y, Schafer J, Farbman AI. Phagocytic cells in the rat olfactory epithelium after bulbectomy. *Exp. Neurol.* 1995;136:225–233.
- Suzuki Y, Takeda M, Farbman AI. Supporting cells as phagocytes in the olfactory epithelium after bulbectomy. *J. Comp. Neurol.* 1996;376: 509–517.
- Tandler B. Structure of mucous cells in salivary glands. *Microsc. Res. Techn.* 1993;26:49–56.
- Tandler B, Phillips CJ. Structure of serous cells in salivary glands. *Microsc. Res. Techn.* 1993;26:32–48.
- Taniguchi K, Toshima Y, Saito TR, Taniguchi K. Development of the Bowman's glands and Jacobson's glands in the Japanese reddy frog, *Rana japonica*. *J. Vet. Med. Sci.* 1996; 58:17–22.
- Wang RT, Halpern M. Scanning electron microscopic studies of the surface morphology of the vomeronasal epithelium and olfactory epithelium of garter snake. *Am. J. Anat.* 1980; 157:399–428.
- Wetzel R. The identification and distribution of recent Xenarthra (Edentata). In: Montgomery GG, ed. *The Ecology and Evolution of Armadillos, Sloths and Vermilinguas*. Washington D.C.: Smithsonian Institution Press, 1985: 5–21.
- Wyllie AH. Glucocorticoid-induced thymocyte apoptosis is associated with endogenous endonuclease activation. *Nature* 1980;284:555–556.
- Yamamoto M. An electron microscopic study of the olfactory mucosa in the bat and the rabbit. *Arch. Histol. Japon.* 1976;35:359–412.
- Young RW. The renewal of photoreceptors cell outer segments. *J. Cell Biol.* 1967;33:61–72.